

Analysis and Modeling of the cerebral development

Julien Lefèvre^{1,2}

¹ LSIS, UMR CNRS 6168, Université d'Aix-Marseille 2

² LNAO, Neurospin, I2BM, CEA Saclay

10 September 2010



Summary

Motivations

Summary

Motivations

Folding Analysis

Summary

Motivations

Folding Analysis

A developmental Model

Summary

Motivations

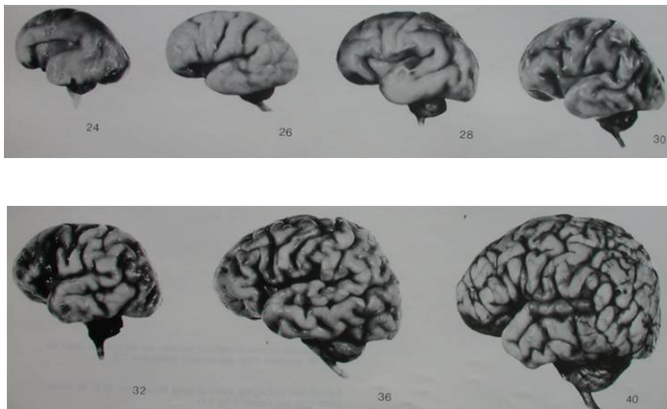
Folding Analysis

A developmental Model

Conclusion

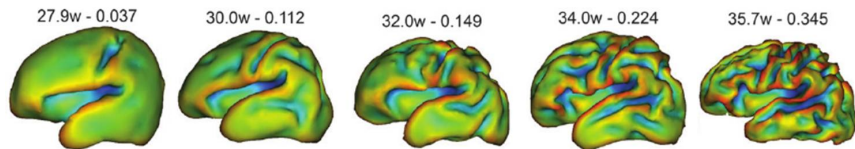
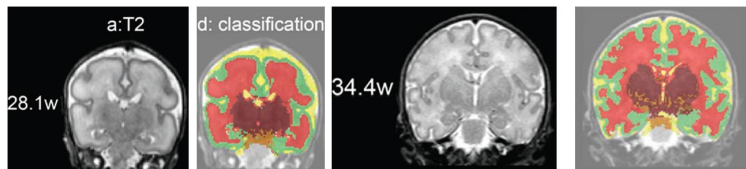
Cortical Development

From 24 weeks to birth : appearance of folding patterns



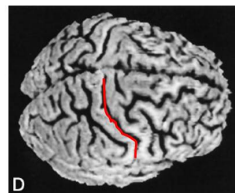
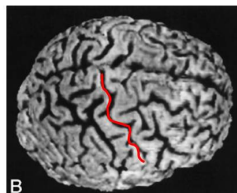
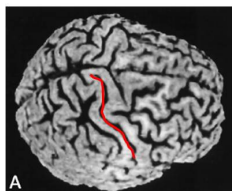
Cortical Development

MRI of premature newborns



Dubois et al,
Cerebral Cortex, 2007

Some questions



Biondi et al,

American Journal of Neuroradiology, 1998

- How does the development shapes the anatomy of the brain ?
- How to explain both reproducibility and variability in the sulcal patterns of the brain ?

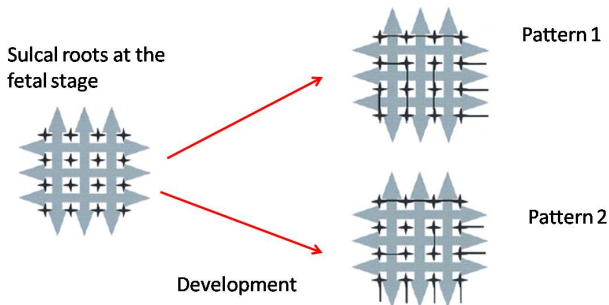
"Sulcal Roots" theory

Anatomical landmarks present among human brains



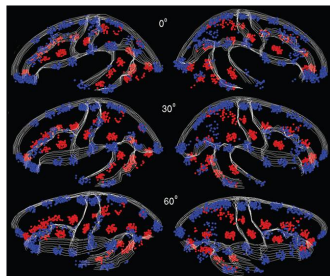
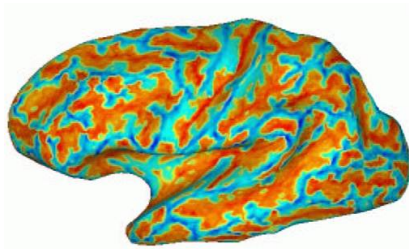
Regis et al,

Neurologia medico-chirurgica, 2005



"Sulcal Roots" theory

Sulcal roots can be identified with mean curvature or depth maps



Cachia et al,
IEEE TMI, 2003



Lohmann et al,
Cerebral Cortex, 2008

Identification of growth seeds

Method to track the origin of the folding process of neonates

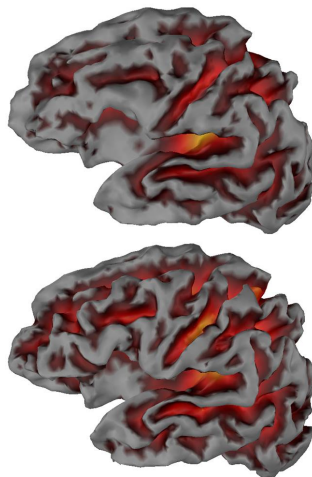


Lefèvre et al,
IPMI, 2009

- **Longitudinal data**
2 T2 MRI of 4 neonates at birth and at birth + 4 weeks
- **Brain segmentation**
- **Depth maps**
- **Non linear Registration**



Cachier et al,
Computer Vision and Image Understanding, 2003



Optical flow computation

- **Minimization of the functional**

$$\mathcal{E}(\mathbf{V}) = \int_{\mathcal{M}} \left(\frac{\partial I}{\partial t} + g(\mathbf{V}, \nabla_{\mathcal{M}} I) \right)^2 d\mu + \lambda \int_{\mathcal{M}} \text{Tr}({}^t \nabla \mathbf{V} \cdot \nabla \mathbf{V}) d\mu$$

- **Variational formulation and finite elements method**

$$f(\mathbf{U}) = - \int_{\mathcal{M}} g(\mathbf{U}, \nabla_{\mathcal{M}} I) \partial_t I d\mu,$$

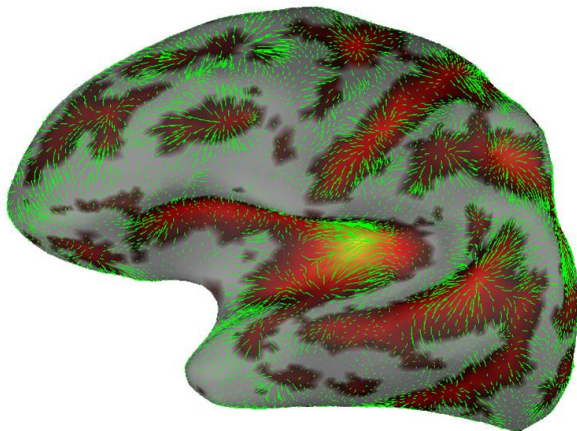
$$a(\mathbf{U}, \mathbf{V}) = \int_{\mathcal{M}} g(\mathbf{U}, \nabla_{\mathcal{M}} I) g(\mathbf{V}, \nabla_{\mathcal{M}} I) d\mu + \lambda \int_{\mathcal{M}} \text{Tr}({}^t \nabla \mathbf{U} \nabla \mathbf{V}) d\mu.$$

$$\mathbf{V} = \arg \min_{\mathbf{U} \in \Gamma^1(\mathcal{M})} \mathcal{E}(\mathbf{U}) \iff a(\mathbf{V}, \mathbf{U}) = f(\mathbf{U}), \forall \mathbf{U} \in \Gamma^1(\mathcal{M})$$



Optical flow computation

- **Results**



Discrete Helmholtz decomposition

Theorem : Given \mathbf{V} a vector field on a mesh \mathcal{M}_h , there exists unique functions U and A , up to an additive constant, and a vector field \mathbf{H} such as :

$$\begin{aligned}\mathbf{V} &= \nabla_{\mathcal{M}_h} U + \mathbf{Curl}_{\mathcal{M}_h} A + \mathbf{H} \\ \operatorname{div}_{\mathcal{M}_h} \mathbf{H} &= 0 \quad \operatorname{curl}_{\mathcal{M}_h} \mathbf{H} = 0\end{aligned}$$

with the following definitions :

$$\int_{\mathcal{M}} U \operatorname{div}_{\mathcal{M}_h} \mathbf{H} = - \int_{\mathcal{M}_h} g(\mathbf{H}, \nabla_{\mathcal{M}_h} U)$$

$$\mathbf{Curl}_{\mathcal{M}_h} A = \nabla_{\mathcal{M}_h} A \wedge \mathbf{n} \quad \operatorname{curl}_{\mathcal{M}_h} \mathbf{H} = \operatorname{div}_{\mathcal{M}_h} (\mathbf{H} \wedge \mathbf{n})$$



Polthier & Preuß,

Visualisation and Mathematics, 2002

Discrete Helmholtz decomposition

U and A minimize the two functionals :

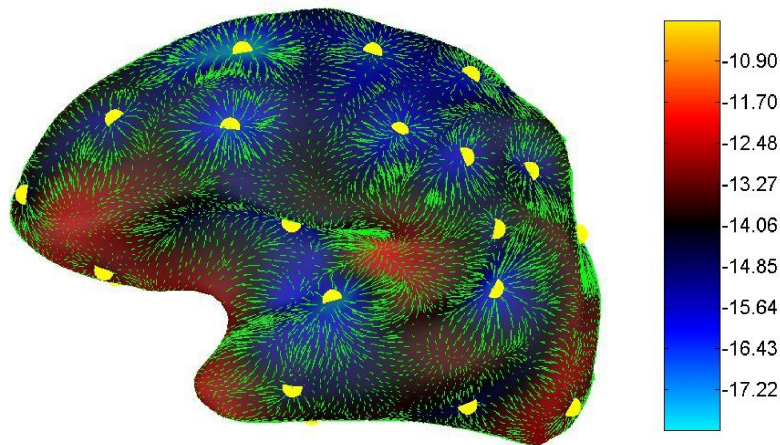
$$\int_{\mathcal{M}} \|\mathbf{V} - \nabla_{\mathcal{M}_h} U\|^2$$
$$\int_{\mathcal{M}} \|\mathbf{V} - \mathbf{Curl}_{\mathcal{M}_h} A\|^2$$

The minima U and A satisfy :

$$\forall \phi, \int_{\mathcal{M}} g(\mathbf{V}, \nabla_{\mathcal{M}_h} \phi) = \int_{\mathcal{M}} g(\nabla_{\mathcal{M}_h} U, \nabla_{\mathcal{M}_h} \phi)$$
$$\forall \phi, \int_{\mathcal{M}} g(\mathbf{V}, \mathbf{Curl}_{\mathcal{M}_h} \phi) = \int_{\mathcal{M}} g(\mathbf{Curl}_{\mathcal{M}_h} A, \mathbf{Curl}_{\mathcal{M}_h} \phi)$$

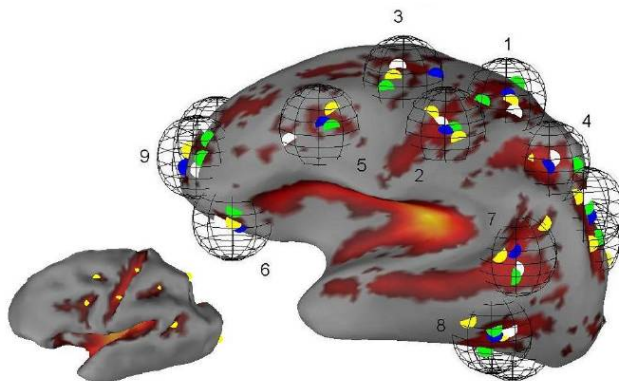
Discrete Helmholtz decomposition

Potential U and its local minima



Identification of growth seeds

9 reproducible clusters of growth seeds among 4 subjects

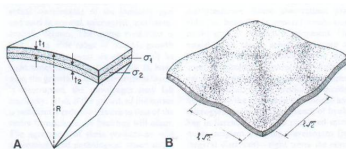


Different hypotheses of the cortical folding

- Differential growth of cortical layers**



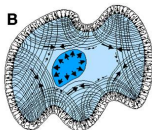
Richman et al,
Science, 1976



- Mechanical tensions exerted by white matter fibers**



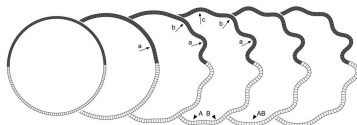
Van Essen,
Nature, 1997



- Elasticity/plasticity of the cortex**



Toro & Burnod,
Cerebral Cortex, 2005



Reaction-diffusion approaches

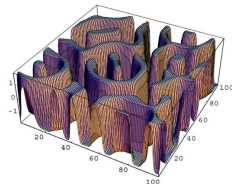
- Morphogenesis**



Turing,
Phil. Trans. Roy. Soc. Lond. B,
1952



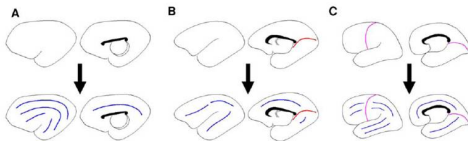
Cartwright,
Journal of Theoretical Biology,
2002



- Prediction of folding orientation**



Striegel & Hurdal,
PLOS Computational
Biology, 2009



Our approach

- Gray-Scott model**

Two interacting morphogens, U (inhibitor) and V (activator).

$$\partial_t U = d_1 \Delta U + F(1 - U) - UV^2$$

$$\partial_t V = d_2 \Delta V + UV^2 - (F + k)V$$

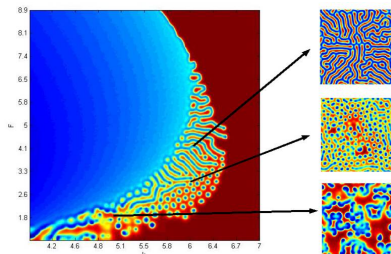
Leads to pattern formation



Pearson,
Science, 1993



McGough & Riley,
Non Linear Analysis, 2004



The model

- **Notations :**

\mathcal{M} : the surface on which evolve the morphogens U and V .

g_t : determinant of the metric tensor associated to \mathcal{M} .

- **Reaction-Diffusion mechanism :**

Gray-Scott model adapted for a time-varying geometry



Lefèvre & Mangin,

PLOS Computational Biology, 2010

$$\partial_t U + U \partial_t \log \sqrt{g_t} = d_1 \Delta_{\mathcal{M}_t} U + F(1 - U) - UV^2$$

$$\partial_t V + V \partial_t \log \sqrt{g_t} = d_2 \Delta_{\mathcal{M}_t} V + UV^2 - (F + k)V$$

- **Surface deformation :**

$$\frac{\partial \mathcal{M}}{\partial t} = h(U, V) \mathbf{N}$$

Numerical implementation

- Variational formulation**

$$\forall W \in H_1(\mathcal{M}), \int_{\mathcal{M}} W \partial_t U d\mu + \int_{\mathcal{M}} W U \partial_t \log \sqrt{g_t} d\mu =$$

$$d_1 \int_{\mathcal{M}} W \Delta U d\mu + \int_{\mathcal{M}} W f(U, V) d\mu$$

Then with Green's formula :

$$\forall W \in H_1(\mathcal{M}), \int_{\mathcal{M}} W \partial_t U d\mu + \int_{\mathcal{M}} W U \partial_t \log \sqrt{g_t} d\mu =$$

$$-d_1 \int_{\mathcal{M}} g(\nabla U, \nabla W) d\mu + \int_{\mathcal{M}} W f(U, V) d\mu$$

Numerical implementation

- **Finite Elements**

Given w_i the basis functions associated to a mesh \mathcal{M}_h , we are looking for a solution

$$U(t, x) = \sum_i U_i(t) w_i(x)$$

and the weak formulation becomes :

$$\begin{aligned} \forall j, \quad \sum_i \frac{dU_i}{dt} \int_{\mathcal{M}_h} w_j w_i + \sum_i U_i \int_{\mathcal{M}_h} w_j w_i \partial_t \log \sqrt{g_t} = \\ -d_1 \sum_i U_i \int_{\mathcal{M}_h} g(\nabla w_i, \nabla w_j) + \int_{\mathcal{M}_h} w_j f \left(\sum_i U_i w_i, \sum_i V_i w_i \right) \end{aligned}$$

Numerical Implementation

- Discretization in time**

Implicit and explicit discretization between t^n and

$t^{n+1} = t^n + \Delta t$:

$$[A] \frac{[U]^{n+1} - [U]^n}{\Delta t} + d_1 [\nabla][U]^{n+1} + [B][U]^{n+1} + [A]f([U]^n, [V]^n) = 0$$

with

$$[A]_{i,j} = \int_{\mathcal{M}_h} w_j(x) w_i(x) dx, \quad [\nabla]_{i,j} = \int_{\mathcal{M}_h} g(\nabla w_i, \nabla w_j) dx$$

$$[B]_{i,j} = \int_{\mathcal{M}_h} w_j(x) w_i(x) \frac{\log \sqrt{g_n} - \log \sqrt{g_{n-1}}}{\Delta t} dx$$

$$f([U]^n, [V]^n)_i = f(U_i(t_n), V_i(t_n))$$

Numerical Implementation

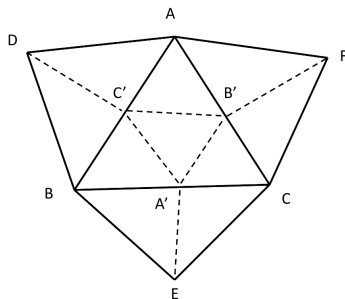
- **Surface deformation**

Each vertex of the mesh is moved according to :

$$v_i^{n+1} = v_i^n + \Delta t h(U_i^{n+1}, V_i^{n+1}) \mathbf{N}_i^n$$

In practice we take
 $h(U, V) = KV$

In order to avoid abnormal deformations, we refine the triangles whose areas exceed a threshold

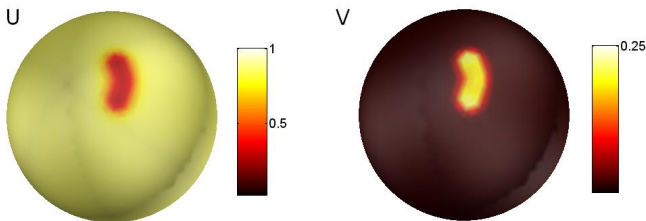


Results

- Labyrinthine Patterns**

$F = 0.04$, $k = 0.06$, $d_1 = 0.2$, $d_2 = 0.1$, $K = 0.0005$ and $\Delta t = 2$.

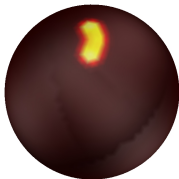
Initial conditions : perturbation of the stable equilibrium $U = 1$, $V = 0$. $U = \frac{1}{2} + n$ and $V = \frac{1}{4} + n$ on a broad line, with n white noise of amplitude 0.001.



Results

- Labyrinthine Patterns**

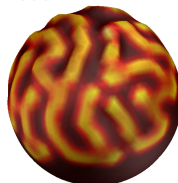
t=1



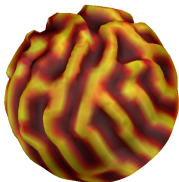
t=1000



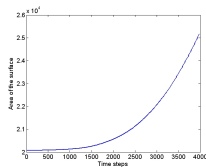
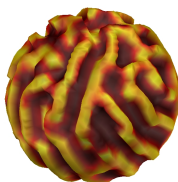
t=2000



t=3000



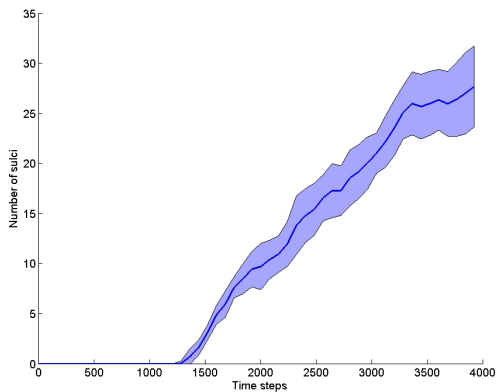
t=4000



Results

- **Order Parameter**

Evolution of the number of folds



Results

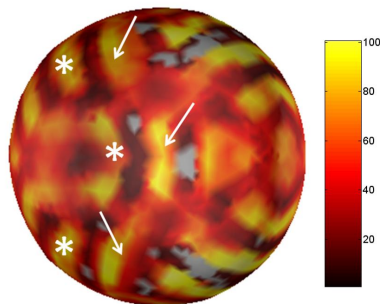
- Reproducibility**

Curvature $\kappa_i(x, t)$ computed for 50 noisy initial conditions.

Folds are defined by $M_i(x, t) = 1_{\kappa_i(x, t) < 0}$

Average map of folding :

$$\sum_{i=1}^{50} M_i(x, 4000)$$



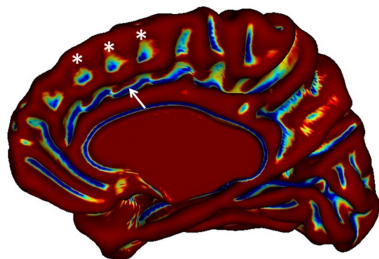
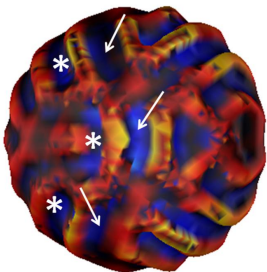
Results

- **Reproducibility**

Comparison with an average model of the cortex



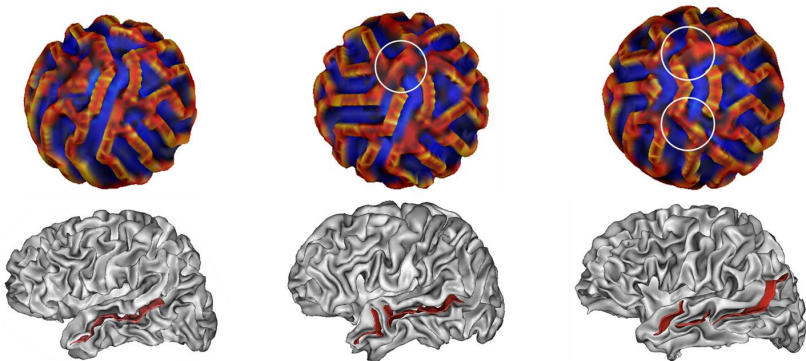
Lyttelton et al,
Neuroimage, 2007



Results

- **Variability**

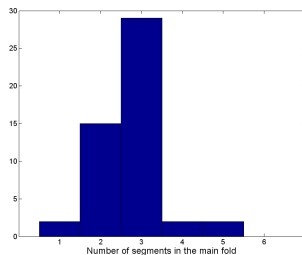
The main fold can be in one or several parts



Results

- **Variability**

Number of connected components in the main fold



Variability of the left STS

1 segment : 28 %

2 segments : 32 %

3 segments : 16 %

4 segments : 24 %

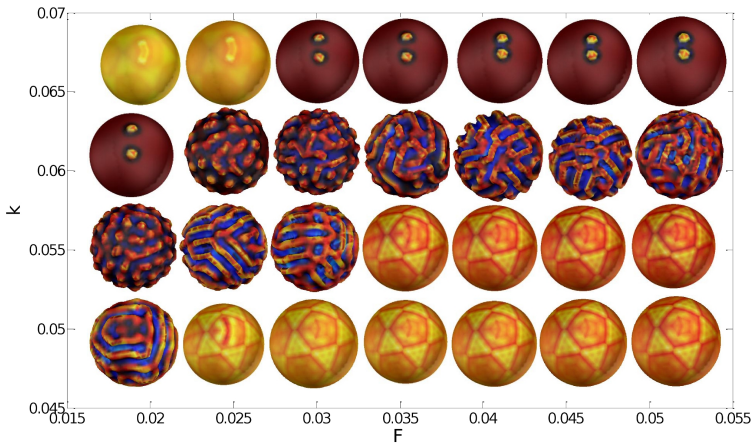


Ochiai et al,

Neuroimage, 2004

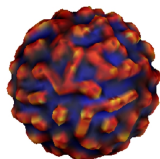
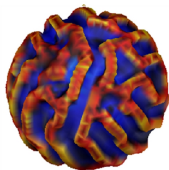
Results

- Phase diagram of the model

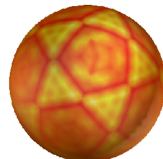


Results

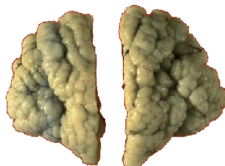
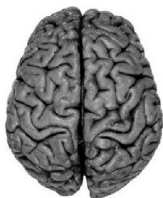
- **Developmental pathologies**



Polymicrogyria



Lissencephaly



Conclusion

- Several qualitative similarities between our "toy model" and the ground truth (reproducibility/variability, phase diagram and pathologies of folding).
- The link between morphogens and genes of cortical development (Pax6, Ngn2, Id4) needs to be explained.
- The effect of surface deformation on pattern formation needs to be studied theoretically.

Aknowledgments

- **LNAO, Neurospin**
Jean-François Mangin
- **INSERM U562, Neurospin**
François Leroy, Jessica Dubois,
- **LENA, CNRS UPR640**
Sylvain Baillet, Sheraz Khan
- **Department of Pediatrics, Geneva University Hospitals**
Petra S. Huppi